CD9 knockdown suppresses cell proliferation, adhesion, migration and invasion, while promoting apoptosis and the efficacy of chemotherapeutic drugs and imatinib in Ph+ ALL SUP-B15 cells

CHONGYUN XING[1,2*], WANLING XU[2*], YIFEN SHI[2*], BIN ZHOU[3], DIJIONG WU[1],
BIN LIANG[2], YUHONG ZHOU[1], SHENMENG GAO[3] and JIANHUA FENG[2,4]

[1]Department of Hematology, The First Affiliated Hospital of Zhejiang Chinese Medical University, Hangzhou,
Zhejiang 310006; [2]Department of Hematology; [3]Laboratory of Internal Medicine; [4]Department of Pediatric
Hematology-Oncology, The First Affiliated Hospital of Wenzhou Medical University, Wenzhou, Zhejiang 325000, P.R. China

Abstract. Philadelphia chromosome-positive acute lympho-blastic leukemia (Ph+ ALL) is regarded as a prognostically unfavorable subgroup, as this ALL subgroup has an increased risk of relapse/refractory disease. CD9, which belongs to the tetraspanin membrane proteins, is implicated in several pathological processes, including tumor progression. However, the role of CD9 in the pathogenesis of Ph+ ALL and the potential benefit of applying CD9-targeted RNA interference strategies for treatment of Ph+ ALL require further investigation. The aim of the present study was to determine the effects of CD9 on leukemic cell progression and the efficacy of therapeutic agents in Ph+ ALL cells, in addition to assessing the *in vitro* anti-leukemia activity of CD9-targeted RNA interference in Ph+ ALL cells. In the present study, a lentiviral short hairpin RNA (shRNA) expression vector targeting CD9 gene in Ph+ ALL SUP-B15 cells was constructed. The present results demonstrated that treatment of SUP-B15 cells with lentiviral-mediated shRNA against CD9 decreased CD9 mRNA and protein expression compared with the shControl cells transduced with a blank vector. In addition, CD9 knockdown could suppress cell proliferation, adhesion, migration and invasion, and promote apoptosis and the efficacy of chemotherapeutic drugs (such as vincristine, daunorubicin, cyclophosphamide and dexamethasone) and the tyrosine kinase inhibitor imatinib in SUP-B15 cells. Furthermore, CD9 knockdown suppressed cell proliferation and promoted apoptosis in SUP-B15 cells via a p53-dependent pathway. These findings suggested that gene silencing of CD9 using a shRNA-expressing lentivirus vector may provide a promising treatment for Ph+ ALL.

Introduction

Acute lymphoblastic leukemia (ALL) is a heterogeneous group of diseases with multiple, prognostically relevant genetic abnormalities and is characterized by over production of abnormal immature white blood cells (1). Philadelphia chromosome-positive (Ph+) ALL is characterized by the existence of a constitutively active breakpoint cluster region-tyrosine-protein kinase ABL1 (BCR-ABL) protein tyrosine kinase, which subverts the transcriptional programs that normally control lymphoid development (2). Ph+ ALL comprises 2-3% of pediatric patients and 20-30% of adult patients with ALL worldwide (3), and this ALL subgroup has been regarded as a prognostically unfavorable subgroup as it has an increased risk of relapse/refractory disease (1,4). Imatinib, a selective inhibitor of the BCR-ABL tyrosine kinase, is effective in treating Ph+ chronic myelogenous leukemia (CML) (5). However, Ph+ ALL is less sensitive to imatinib than CML (6). Thus, there is an urgent requirement to develop novel strategies to treat Ph+ ALL.

CD9, which belongs to the tetraspanin membrane proteins, is expressed in a variety of different types of blood cells, including precursor B-lymphocytes (7). CD9 plays crucial roles in a wide range of physiological processes, including cell motility and fertilization (8). CD9 is also expressed in numerous solid cancer types, including prostate carcinoma, melanoma and glioblastoma, and serves a role in several pathological processes, including cancer cell motility, invasiveness and proliferation (9-15). Previous studies have been conducted to investigate the association between CD9 and ALL with respect to the biological and clinical characteristics. For example, Nishida *et al* (16) and Yamazaki *et al* (17) identified

Correspondence to: Dr Jianhua Feng, Department of Hematology, The First Affiliated Hospital of Wenzhou Medical University, 2 Fuxue Road, Wenzhou, Zhejiang 325000, P.R. China
E-mail: wzfjh@126.com

Dr Shenmeng Gao, Laboratory of Internal Medicine, The First Affiliated Hospital of Wenzhou Medical University, 2 Fuxue Road, Wenzhou, Zhejiang 325000, P.R. China
E-mail: gaoshenmeng77@126.com

*Contributed equally

that CD9+ B-cell ALL (B-ALL) cells exhibited an asymmetric cell division-like proliferation with greater leukemogenic potential than CD9- cells, while CD9+ B-ALL cells exhibited drug-resistance. In addition, an anti-CD9 monoclonal antibody has an anti-proliferative effect on B-ALL cells, and knockdown of CD9 expression suppresses the leukemogenic potential of the B-ALL cell line (17). Thus, these findings suggested that targeted therapies against CD9 may be a novel therapeutic approach for B-ALL. Moreover, Arnaud et al (18) identified that CD9 promoted Ras-related C3 botulinum toxin substrate 1 (RAC1) activation and enhanced C-X-C motif chemokine receptor 4-mediated B-ALL cell migration and engraftment to the bone marrow or testis. Recently, Liang et al (19) revealed that patients with CD9+ ALL exhibited a higher positive rate of the BCR-ABL fusion gene compared with patients who were CD9-, and CD9 expression indicated an poor prognosis in patients with ALL. However, the role of CD9 in the pathogenesis of Ph+ ALL and the potential benefit of applying loss-of-function strategies targeting CD9 for treatment of Ph+ ALL require further examination.

Therefore, the aims of the present study were: i) To determine the effects of CD9 on leukemic cell progression and the efficacy of therapeutic agents in Ph+ ALL cells; and ii) to assess the *in vitro* anti-leukemia activity of CD9-targeted RNA interference in Ph+ ALL cells.

Materials and methods

Cell lines and culture conditions. The human Ph+ ALL cell line SUP-B15 and human embryonic kidney cell line 293T were purchased from The American Type Culture Collection. The SUP-B15 cell line has been authenticated by short tandem repeat DNA profiling analysis by Genetic Testing Biotechnology Corporation (Suzhou). SUP-B15 cells were cultured in Iscove's modified Dulbecco's medium (IMDM; Sigma-Aldrich; Merck KGaA) with 20% FBS (Gibco; Thermo Fisher Scientific, Inc.), and 293T cells were cultured in DMEM (Sigma-Aldrich; Merck KGaA) with 10% FBS. All cells were maintained in a humidified incubator at 37°C in an atmosphere of 5% CO_2.

Lentiviral vector construction and transduction. A total of three interference sequences, shCD9-1, shCD9-2 and shCD9-3, that target human CD9 mRNA (NCBI reference sequence NM_001330312.1; Gene ID 928) were designed with an online small interfering RNA tool (http://bioinfo.clontech.com/rnaidesigner/frontpage.jsp; Clontech Laboratories, Inc.). Primer Designer™ Tool (Invitrogen; Thermo Fisher Scientific, Inc.) was used to design the short hairpin RNA (shRNA) primers for targeting the gene interference sequences of CD9. The primer sequences used in the present study are presented in Table I. The single-stranded oligonucleotides of the sequences were chemically synthesized, annealed to form double-stranded DNA and then inserted into the PHY-310 lentiviral vector [hU6-MCS-CMV-ZsGreen1-PGK-Puro; Han Yin Biotechnology (Shanghai) Co., Ltd.; Fig. 1A], which expresses ZsGreen1 fluorescent protein as a cell-tracking marker, to produce the recombinant shRNA-expressing lentivirus vectors: PHY-310/shCD9-1, PHY-310/shCD9-2 and PHY-310/shCD9-3.

Transduction of SUP-B15 cells with the recombinant lentivirus was performed as described previously (20). Briefly, the subconfluent 293T cells ($1.5x10^8$/dish) in a 10-cm culture dish were co-transfected with 12 μg lentiviral vector and 9 μg lentiviral packaging vector LV-PV001 [Han Yin Biotechnology (Shanghai) Co., Ltd.] using polyethylenimine (Sigma-Aldrich; Merck KGaA). At 48 h after transfection, lentiviral particles were harvested and purified by ultra-centrifugation at 3,000 x g for 2.5 h at 4°C. The viral titer was determined by hole-dilution method (21). SUP-B15 cells ($5x10^5$/well) were seeded into 6-well plates. The lentiviral particles produced from the transfected 293T cells were used to transduce SUP-B15 cells in the presence of 8 μg/ml polybrene (Sigma-Aldrich; Merck KGaA). In the shControl group, SUP-B15 cells were transduced with a blank vector. After 72 h of transduction, fluorescence microscopy (magnification, x200) was used to detect the transduction efficiency, and the efficiency of CD9 knockdown was evaluated by reverse transcription-quantitative PCR (RT-qPCR) and western blotting, as well as flow cytometry analysis. After 96 h of transduction, the transduced SUP-B15 cells were used for subsequent experiments.

RT-qPCR assay. Total RNA in the SUP-B15 cells was isolated using TRIzol® reagent (Invitrogen; Thermo Fisher Scientific, Inc.). Total RNA was reverse transcribed into cDNA using the ExScript RT reagent kit (Takara Bio, Inc.) at 37°C for 15 min. qPCR was performed as previously described (20). PCR primers were designed for amplifying DNA fragments that span intron-exon boundaries, and the primer sequences were as follows: CD9 forward, 5'-TCGCCATTGAAATAGCTGCGG C-3' and reverse, 5'-CGCATAGTGGATGGCTTTCAGC-3'; and ribosomal protein L13a forward, 5'-CGAGGTTGGCTG GAAGTACC-3' and reverse 5'-CTTCTCGGCCTGTTTCCG TAG-3'. qPCR was subsequently performed in the ABI 7500 real-time PCR machine (Applied Biosystems; Thermo Fisher Scientific, Inc.) using a SYBR-Green PCR Master Mix (Takara Bio, Inc.). The following thermocycling conditions were used for the qPCR: Initial denaturation at 95°C for 5 min; followed by 40 cycles of denaturation at 95°C for 10 sec and combined annealing/extension at 60°C for 20 sec. Ribosomal protein L13a was used as an internal control and the relative gene expression levels were calculated using the $2^{-\Delta\Delta Cq}$ method (22).

Western blotting. The methods of protein extraction and western blot analysis were carried out according to a previous study (20). Briefly, cells were lysed with RIPA lysis buffer (Beyotime Institute of Biotechnology) and the total protein concentration was determined using a BCA protein assay kit (Beyotime Institute of Biotechnology). Total protein (30 μg/lane) was separated by 10% SDS-PAGE and then transferred to a PVDF membrane. The membranes were blocked with 5% skim-milk diluted in TBS-0.1% Tween-20 for 1 h at room temperature, and then the blots were incubated overnight with primary antibodies at 4°C. The primary antibodies used were anti-p53 (1:1,000, cat. no. 9282, Cell Signaling Technology, Inc.), anti-p21 (1:1,000, cat. no. 2947, Cell Signaling Technology, Inc.), anti-caspase 3 (1:1,000, cat. no. 9662, Cell Signaling Technology, Inc.), anti-cleaved caspase 3 (1:1,000, cat. no. 9579, Cell Signaling Technology, Inc.), anti-CD9 (1:1,000, cat. no. 20597-1-AP, ProteinTech

Table I. Primers used for targeting the interference sequences of the CD9 gene.

Primer	Primer sequence (5'-3')
shCD9-1	F: GATCCGCGGGAAACGCTGAAAGCCATTCAAGAGATGGCTTTCAGCGTTTCCCGTTTTTTG
	R: AATTCAAAAAACGGGAAACGCTGAAAGCCATCTCTTGAATGGCTTTCAGCGTTTCCCGCG
shCD9-2	F:GATCCGCCACAAGGATGAGGTGATTAGAGAACTTAATCACCTCATCCTTGTGGTTTTTTG
	R: AATTCAAAAAACCACAAGGATGAGGTGATTAAGTTCTCTAATCACCTCATCCTTGTGGCG
shCD9-3	F:GATCCAGGAAGTCCAGGAGTTTTATTCAAGAGATAAAACTCCTGGACTTCCTTTTTTTG
	R: AATTCAAAAAAGGAAGTCCAGGAGTTTTATCTCTTGAATAAAACTCCTGGACTTCCTG

F, forward; R, reverse; sh, short hairpin RNA.
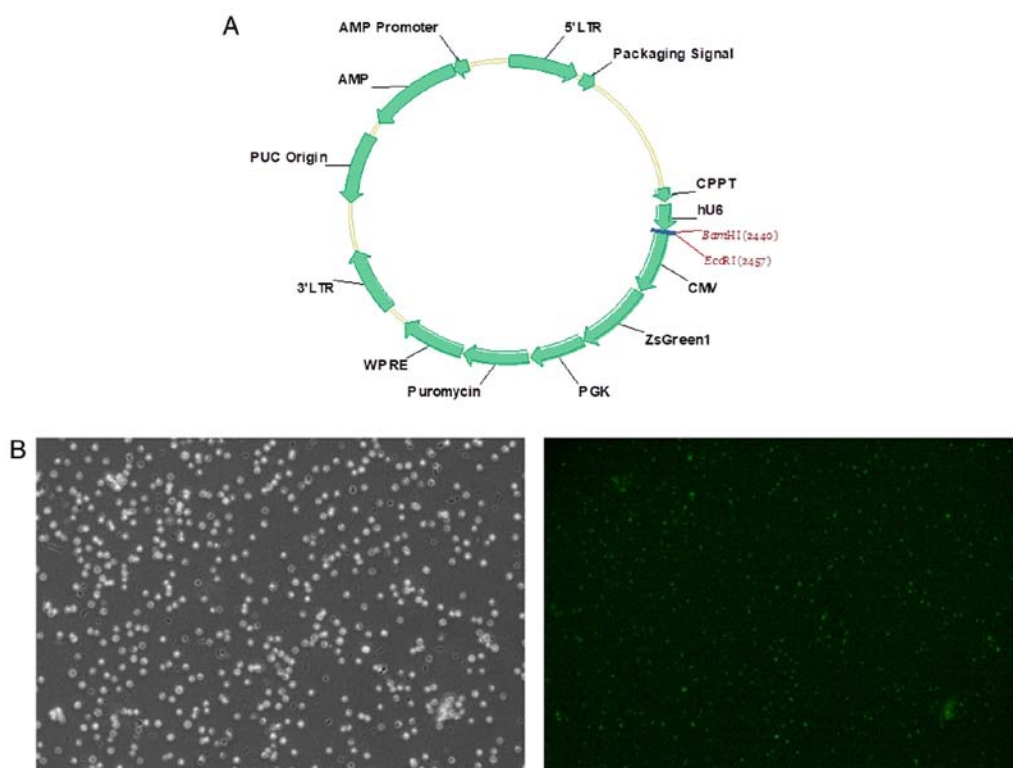
Figure 1. Successful transduction of SUP-B15 cells with a lentiviral vector containing shRNA targeting CD9. (A) PHY-310 lentiviral vector: hU6-MCS-CMV-ZsGreen1-PGK-Puro. (B) Detection of lentiviral transduction efficiency. SUP-B15 cells were transduced with PHY-310/shCD9-3. Bright (left) and ZsGreen1 fluorescent protein (right) images were obtained 72 h after transduction (magnification, x100). sh/shRNA, short hairpin RNA.

Group, Inc.) and anti-β-actin (1:3,000, cat. no. 4970, Cell Signaling Technology, Inc.). Following incubation using horseradish peroxidase-conjugated anti-rabbit antibody (1:10,000, cat. no. A6154, Sigma-Aldrich; Merck KGaA) or anti-rat antibody (1:10,000, cat. no. A5795, Sigma-Aldrich; Merck KGaA) at room temperature for 1 h, the protein bands were analyzed with a freshly prepared enhanced chemiluminescent solution (GE Healthcare Life Sciences). The relative density of protein expression was quantified using ImageJ software (version 1.49p; National Institutes of Health). Protein levels were standardized against β-actin.

To investigate the effect of CD9 blockade on the expression of p53 and p53-related proteins, SUP-B15 cells ($5x10^5$) were untreated or treated with the IgG isotype control (cat. no. 2729S, Cell Signaling Technology, Inc.) or anti-CD9 antibody (at a concentration of 50 μg/ml; cat. no. 20597-1-AP; Protein Tech Group, Inc.) at 37°C for 24 h, and then were lysed and subjected to western blot analysis.

Flow cytometry assay. To detect the membrane expression of CD9, $3x10^5$ cells were harvested and treated with Fc Block (1:100; BD Biosciences) for 15 min at 4°C. Thereafter, the cell surface was stained with phycoerythrin (PE)-conjugated anti-CD9 (1:50; cat. no. 12-0098-41; eBioscience; Thermo Fisher Scientific, Inc.) for 30 min at 4°C. PE-conjugated mouse IgG1 κ isotype control (1:50; cat. no. 12-4714-82; eBioscience; Thermo Fisher Scientific, Inc.) was used as a negative control. The membrane expression of CD9 in SUP-B15 cells was then analyzed using a FACSCalibur flow cytometer (BD Biosciences) and FlowJo version 10 software (FlowJo LLC).

Cell proliferation assay. Cell Counting Kit-8 (CCK-8; Dojindo Molecular Technologies, Inc.) was used for a cell proliferation assay, according to the manufacturer's protocol. Cells were cultured in 96-well plates at a concentration of $3x10^3$ cells/well. After incubation at 37°C for 24, 48, 72 and 96 h, CCK-8 solution (10 µl) was added to each well and cells were incubated for 2 h at 37°C. The absorbance was detected at 450 nm using a SpectraMax M5 microplate reader (Molecular Devices, LLC).

Apoptosis assay. Allophycocyanin-labeled Annexin V (BD Biosciences) and DAPI (BD Biosciences) double staining (both stained at room temperature for 15 min) was used to detect early and late apoptosis. The cells were analyzed using a FACSCalibur flow cytometer (BD Biosciences) and FlowJo version 10 software (FlowJo LLC). Annexin V-positive cells were defined as apoptotic.

To investigate the effect of the caspase 3 inhibitor in combination with CD9 knockdown on apoptosis, cells were preincubated with 0.6 µmol/l Z-DEVD-FMK (MedChemExpress) at 37°C for 24 h prior to the apoptosis assay.

Cell cycle assay. Cells were washed with PBS, treated with 0.1 mg/ml RNAse A at 37°C for 30 min, stained with propidium iodide (0.05 mg/ml; Invitrogen; Thermo Fisher Scientific, Inc.) at 37°C for 1 h, and then analyzed using a FACSCalibur flow cytometer (BD Biosciences). Multicycle version 4.0 software (Phoenix Flow Systems, Inc.) was used for calculating the cell cycle phase distribution from the resultant DNA histogram.

Drug sensitivity assay. In vitro drug sensitivity to therapeutic agents was assessed with CCK-8 as previously described (20). Cells were exposed to different concentration gradients of chemotherapeutic agents [including vincristine (VCR; 10, 20, 30, 40 and 50 µg/l; Selleck Chemicals), daunorubicin (DNR; 10, 20, 30, 40 and 50 µg/l; Selleck Chemicals), cyclophosphamide (CPM; 50, 100, 200, 400, 600, 800 and 1,000 µg/ml; Selleck Chemicals), dexamethasone (DXM; 0.5, 1, 1.5, 2 and 2.5 nmol/l; Selleck Chemicals) or imatinib (10, 20 and 30 µmol/l; Sigma-Aldrich; Merch KGaA) at 37°C for 48 h, and CCK-8 was used to determine the cell viability. Optical density (OD) values were measured at 450 nm using a SpectraMax M5 microplate reader (Molecular Devices, LLC). The cytotoxicity was calculated using the following formula: Cytotoxicity (%)=(1-mean OD of treated/mean OD of control) x100.

Cell adhesion assay. An artificial basement membrane used for the cell adhesion assay was prepared by adding 0.5 µg Superfibronectin (Sigma-Aldrich; Merck KGaA) into each well of a 96-well plate and incubating at 4°C overnight. Subsequently, $1x10^5$ SUP-B15 cells/well were seeded into the 96-well plate and allowed to adhere to the Superfibronectin at 37°C for 90 min in a humidified incubator with an atmosphere of 5% CO_2. Non-adherent cells were then carefully removed by rinsing with PBS. Finally, adherent cells were quantified by CCK-8 using the same method described previously.

Cell migration and invasion assays. In the cell migration assay, a total of $1x10^4$ SUP-B15 cells suspended in 100 µl serum-free IMDM (Sigma-Aldrich; Merck KGaA) was placed in the upper chamber of a 8-µm pore size Transwell plate (Corning, Inc.) and 800 µl IMDM containing 10% FBS (Gibco; Thermo Fisher Scientific, Inc.) was added to the bottom chamber as a chemoattractant. After incubation for 72 h at 37°C and 5% CO_2 atmosphere, cells that migrated to the bottom chamber were fixed in 4% paraformaldehyde at room temperature for 20 min, stained with 1% crystal violet at room temperature for 30 min, and then counted using a hemocytometer under a light microscope (magnification, x100). The invasion assay was performed by the same procedure except that the upper chamber was coated with 50 µl Matrigel (1 mg/ml; BD Biosciences) at 37°C for 5 h.

In addition, in order to assess the effect of CD9 blockade on adhesion, migration and invasion of Ph+ ALL cells, SUP-B15 cells ($2.5x10^4$) were untreated or treated with the IgG isotype control or anti-CD9 antibody (10 µg/ml) at 37°C for 4 h before cell adhesion, migration and invasion assays were performed.

Statistical analysis. Data are presented as the mean ± standard deviation from three individual experiments. The statistical significance of differences among groups was assessed with one-way ANOVA followed by Tukey's post-hoc test for multiple comparisons. $P<0.05$ was considered to indicate a statistically significant difference. All statistical analyses were performed with Stata software (version 12.0; StataCorp LP).

Results

Downregulation of CD9 mRNA and protein expression in SUP-B15 cells using a lentivirus-based approach. In order to establish an efficient method of permanent knockdown of CD9 in SUP-B15 cells, a lentiviral-mediated shRNA approach was used. To demonstrate the delivery efficiency of shRNA, the SUP-B15 cells were transduced with PHY-310, PHY-310/shCD9-1, PHY-310/shCD9-2 and PHY-310/shCD9-3 carrying the ZsGreen1 gene. Successful lentiviral transduction was demonstrated by fluorescence microscopy after transduction for 72 h (Fig. 1B). Lentiviral delivery of shRNA targeted against CD9 led to a downregulation of CD9 mRNA in SUP-B15 cells, to 2.51±3.00% in the PHY-310/shCD9-1 group, 8.83±1.41% in the PHY-310/shCD9-2 group and 73.51±3.22% in the PHY-310/shCD9-3 group, compared with the shControl group, as measured by RT-qPCR (Fig. 2A). Based on maximal mRNA inhibition of CD9 in the PHY-310/shCD9-3 group, PHY-310/shCD9-3 was utilized for the subsequent experimental paradigms. The protein expression of CD9 in
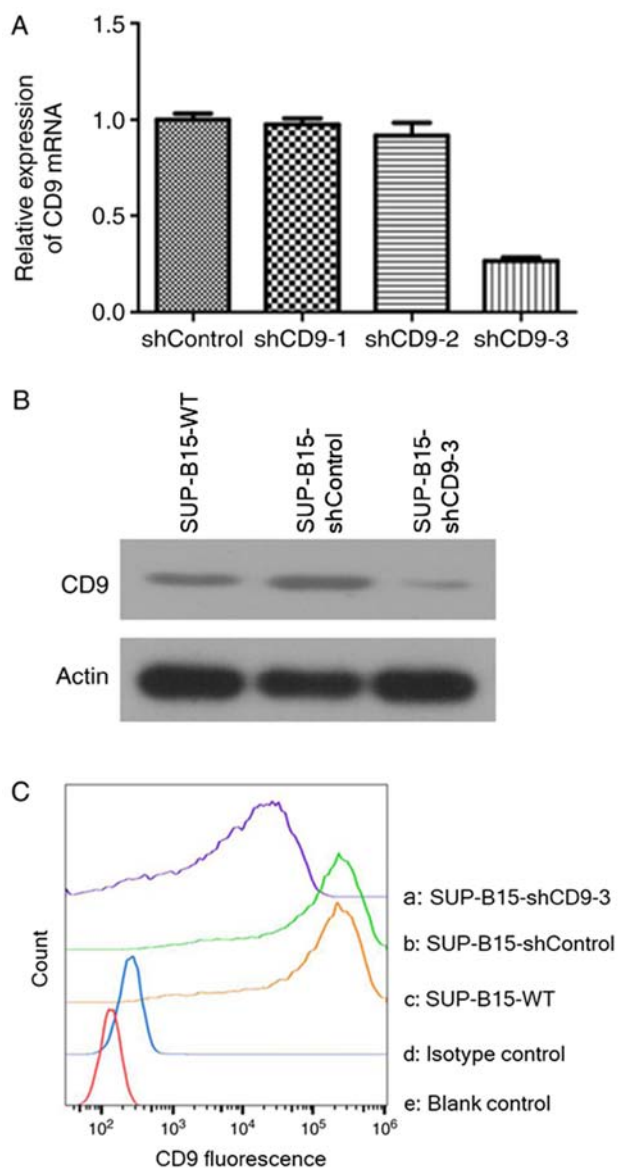
Figure 2. Treatment of SUP-B15 cells with lentiviral-mediated CD9 shRNA reduces CD9 mRNA and protein expression. (A) Analysis of the mRNA expression of CD9 in the SUP-B15 cells transduced with shControl, PHY-310/shCD9-1, PHY-310/shCD9-2 or PHY-310/shCD9-3 by reverse transcription-quantitative PCR. Data are presented as the mean ± SD of three independent experiments. (B) Analysis of CD9 protein expression in the SUP-B15 cells transduced with shControl or PHY-310/shCD9-3 by western blotting. (C) CD9 expression at the cell surface was measured by flow cytometry. Membrane expression of CD9 in shCD9-3, shControl and SUP-B15-WT groups is represented by line a, b and c, respectively. Line d represents the PE-conjugated isotype control in the SUP-B15-WT group. Line e represents the blank control without PE-conjugated anti-CD9 or PE-conjugated isotype control in the SUP-B15-WT group. Fluorescence intensity is represented by the horizontal axis. sh, short hairpin RNA; WT, wild-type; PE, phycoerythrin.

the stably transduced SUP-B15 cells after PHY-310/shCD9-3 transduction is presented in Fig. 2B. The results suggested that PHY-310/shCD9-3 induced a marked downregulation of the CD9 protein expression compared with the SUP-B15-wild-type (WT) and shControl groups.

The membrane expression of CD9 was measured by flow cytometry. Transduction with PHY-310/shCD9-3 resulted in notable reduction of the mean fluorescence intensity of the CD9 molecule in SUP-B15 cells compared with the SUP-B15-WT

(89.9% reduction) and shControl groups (90.2% reduction; Fig. 2C). These results suggested that lentiviral-mediated delivery of shRNA targeting the CD9 gene was able to markedly downregulate the expression of CD9 mRNA and protein in SUP-B15 cells.

Silenced CD9 inhibits cell proliferation, promotes apoptosis and arrests the cell cycle in SUP-B15 cells. In order to evaluate the impact of silenced CD9 on SUP-B15 cell survival, the CCK-8 assay and flow cytometry were used to analyze cell proliferation and apoptosis, respectively. From the CCK-8 assay, it was identified that the proliferation of cells transduced with CD9-shRNA was significantly reduced after 96 h of incubation compared with the SUP-B15-WT and shControl groups (Fig. 3A). The study examined whether the attenuated proliferation of SUP-B15 cells with CD9 knockdown was associated with an increase in apoptosis. SUP-B15 apoptosis was evaluated by flow cytometry analysis with CD9 knockdown cells, together with treatment with caspase 3 inhibitor Z-DEVD-FMK (MedChem Express). Flow cytometry results demonstrated that knockdown of CD9 significantly increased apoptosis compared with the SUP-B15-WT and shControl groups (Fig. 3B). However, pre-treatment with 0.6 μmol/l Z-DEVD-FMK for 24 h prior to apoptosis assay ameliorated CD9 knockdown-induced apoptosis of SUP-B15 cells. These findings suggested that apoptosis in CD9-knockdown cells may be regulated via caspase-dependent pathways.

To determine whether CD9 knockdown has an effect on the cell cycle, the DNA content of SUP-B15 cells was analyzed by flow cytometry. Cell cycle analysis demonstrated that silencing of CD9 significantly increased the percentage of cells in the G_2/M phase, but decreased cells in G_0/G_1 and S phases (Fig. 3C). Therefore, it was speculated that CD9 knockdown was able to arrest cell cycle progression in SUP-B15 cells.

Silenced CD9 increases the cytotoxicity of therapeutic agents in SUP-B15 cells. To assess the potential functional significance of CD9 in chemotherapeutic resistance of Ph+ ALL cells, the impact of CD9 knockdown in SUP-B15 cells on their susceptibility to chemotherapeutic agent-induced cytotoxicity was investigated. Different concentration gradients of chemotherapeutic drugs (such as VCR, DNR, CPM and DXM) were incubated with SUP-B15 cells for 48 h, and then, the CCK-8 assay was used to determine the cytotoxicity. Silencing of CD9 significantly increased the susceptibility of SUP-B15 cells to the cytotoxicity of VCR (Fig. 4A), DNR (Fig. 4B), CPM (Fig. 4C) and DXM (Fig. 4D). In addition, whether CD9 knockdown in SUP-B15 cells increased the cytotoxicity of the BCR-ABL tyrosine kinase inhibitor imatinib was assessed. A concentration gradient of imatinib was used to treat SUP-B15 cells. The results demonstrated that silencing of CD9 also significantly increased the cytotoxicity of imatinib in SUP-B15 cells (Fig. 4E).

Silenced CD9 inhibits adhesion, migration and invasion of SUP-B15 cells. Invasion and metastasis are key clinicopathological features of acute leukemia (23). Thus, whether CD9 knockdown affected cell adhesion, migration and invasion in SUP-B15 cells was analyzed. The results indicated that CD9-silenced SUP-B15 cells exhibited less potential of
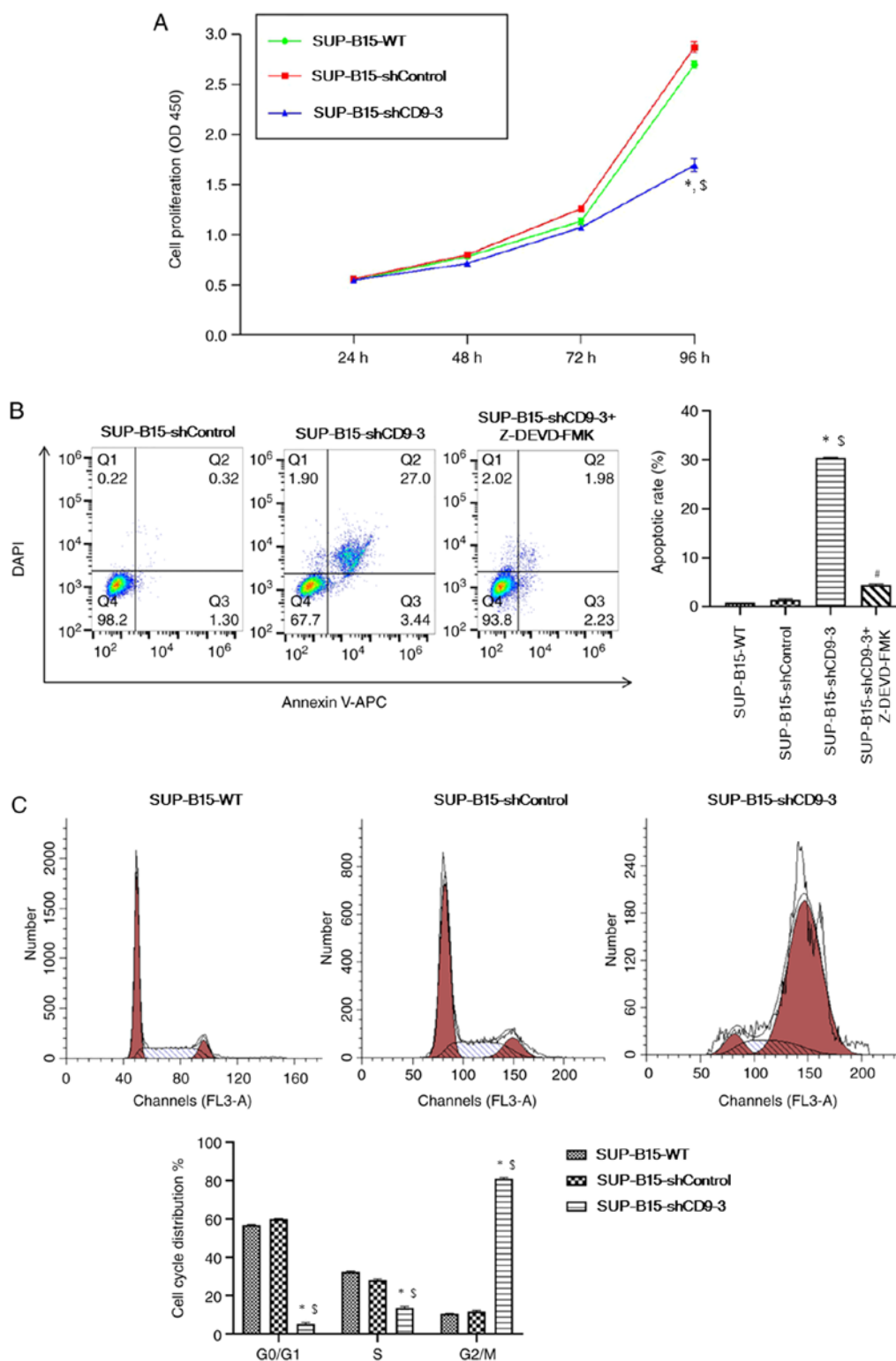
Figure 3. CD9 knockdown suppresses proliferation, promotes apoptosis and induces G_2/M cell cycle arrest in SUP-B15 cells. (A) Cell proliferation curves of SUP-B15 cells were measured by a Cell Counting Kit-8 assay. (B) SUP-B15 apoptosis was determined using flow cytometry analysis. The rate of apoptosis (Annexin-V^+ cells) in SUP-B15 cells was quantified. Treatment with caspase 3 inhibitor Z-DEVD-FMK ameliorated CD9 knockdown-induced apoptosis of SUP-B15 cells. (C) Flow cytometric analysis of cell cycle distribution of SUP-B15 cells. *$P<0.05$ vs. SUP-B15-WT group; $^$P<0.05$ vs. shControl group; #$P<0.05$ vs. shCD9-3 group without Z-DEVD-FMK treatment. sh, short hairpin RNA; WT, wild-type; APC, allophycocyanin; OD, optical density.

adhesion (Fig. 5A), migration (Fig. 5B) and invasion (Fig. 5C) compared with the SUP-B15-WT and shControl cells. In addition, in order to verify the effect of CD9 knockdown on adhesion, migration and invasion of Ph$^+$ ALL cells, SUP-B15 cells were incubated with anti-CD9 antibody before cell adhesion, migration and invasion assays were performed. It was found that anti-CD9 antibody-treated SUP-B15 cells exhibited significantly less potential of adhesion (Fig. 5D), migration (Fig. 5E) and invasion (Fig. 5F) compared with the untreated cells and IgG isotype-treated control cells.
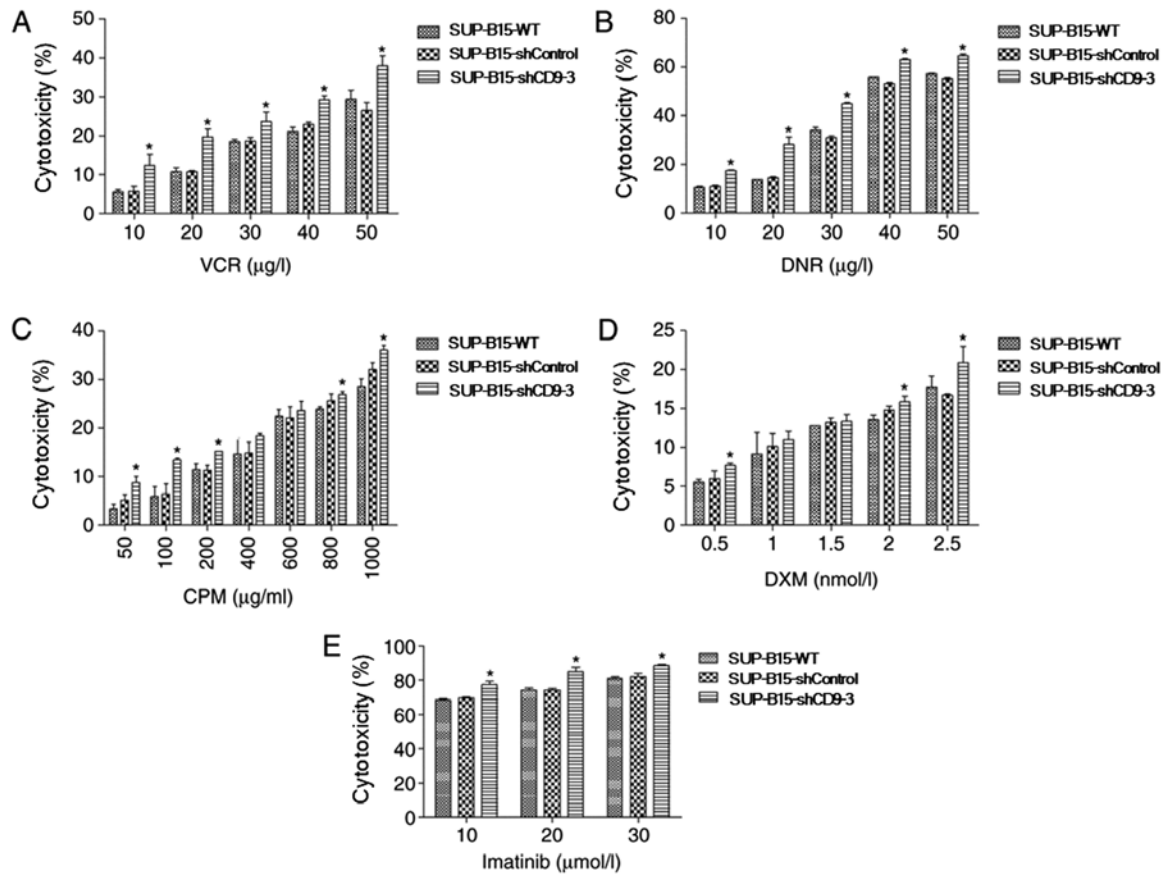
Figure 4. CD9 knockdown promotes the cytotoxicity efficacy of chemotherapeutic drugs and imatinib in SUP-B15 cells. SUP-B15 cells were treated with different concentration gradient of (A) VCR, (B) DNR, (C) CPM, (D) DXM and (E) imatinib for 48 h. Cell Counting Kit-8 assay was used to measure cell viability. *P<0.05 vs. shControl group. VCR, vincristine; DNR, daunorubicin; CPM, cyclophosphamide; DXM, dexamethasone; sh, short hairpin RNA; WT, wild-type.
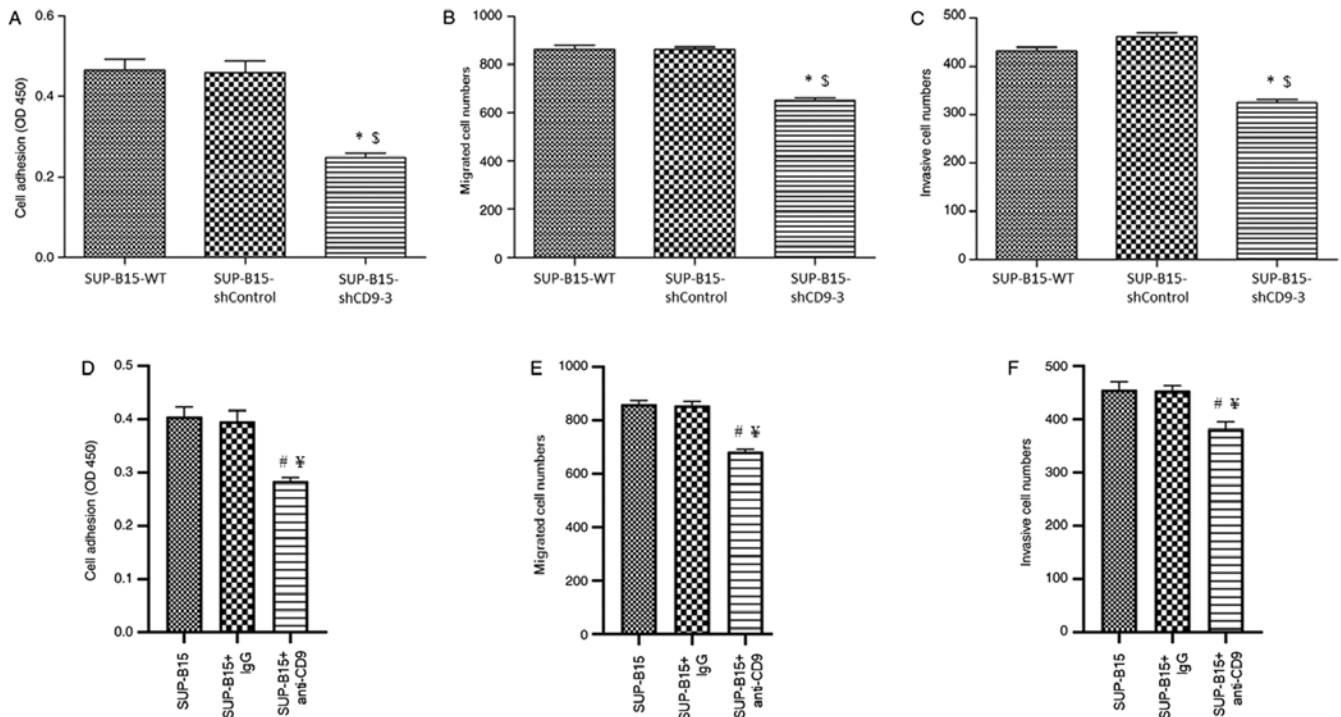
Figure 5. CD9 knockdown or antibody-mediated blockade of CD9 inhibits the adhesion, migration and invasion of SUP-B15 cells. CD9 knockdown suppressed SUP-B15 (A) cell adhesion, (B) migration and (C) invasion. Antibody-mediated blockade of CD9 suppresses SUP-B15 (D) cell adhesion, (E) migration and (F) invasion. *P<0.05 vs. SUP-B15-WT group; $P<0.05 vs. shControl group; #P<0.05 vs. untreated group; ¥P<0.05 vs. IgG isotype-treated group. sh, short hairpin RNA; OD, optical density.
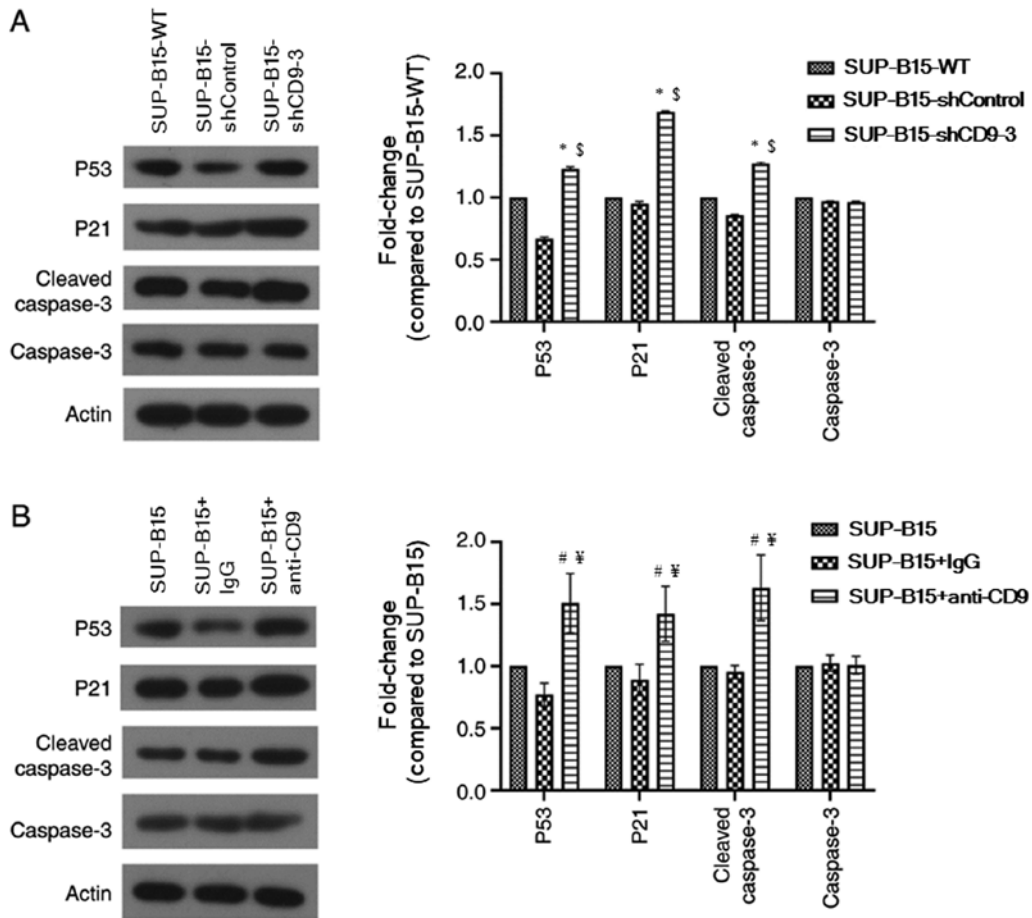
Figure 6. CD9 knockdown or antibody-mediated blockade of CD9 increases the expression of p53, p21 and cleaved caspase 3 proteins. Expression levels of proliferation- and apoptosis-related proteins in SUP-B15 cells were determined by western blotting and densitometric analyses after (A) CD9 knockdown or (B) antibody-mediated blockade of CD9. β-actin was used as the loading control. Densitometry results are expressed as fold-change against untreated control, normalized to the density of the corresponding β-actin band. $^{*}P<0.05$ vs. SUP-B15-WT group; $^{\$}P<0.05$ vs. shControl group; $^{\#}P<0.05$ vs. untreated group; $^{¥}P<0.05$ vs. IgG isotype-treated group. WT, wild-type; sh, short hairpin RNA.

Silenced CD9 inhibits SUP-B15 cell proliferation and promotes apoptosis via a p53-dependent pathway. To identify the potential mechanism via which knockdown of CD9 suppresses proliferation and induces apoptosis in SUP-B15 cells, the expression levels of proliferation- and apoptotic-related proteins (such as p53, p21 and cleaved caspase 3) were detected using western blotting (Fig. 6A). Compared with the SUP-B15-WT and shControl groups, p53 and p21 protein expression levels were significantly increased in the CD9 shRNA group. In addition, silenced CD9 promoted cleaved caspase 3 protein expression. These findings suggested that silenced CD9 inhibited SUP-B15 cell proliferation and promoted apoptosis via a p53-dependent pathway.

Whether CD9 blockade may affect the expression of p53 and p53-related proteins was also investigated. The results suggested that p53, p21 and cleaved caspase 3 protein expression levels were significantly increased in the anti-CD9-treated SUP-B15 cells compared with the untreated cells and IgG isotype-treated cells (Fig. 6B).

Discussion

It is well known that the expression of CD9 fluctuates during B cell development. For instance, precursor B cells have high

CD9 expression, mature B cells display downregulation of CD9 and plasma cells re-express CD9 (24). Previous studies conducted by Nishida *et al* (16) and Yamazaki *et al* (17) reported that CD9 may be a marker for the identification of leukemic stem cells in B-ALL, and that CD9 may regulate cancer stem cell function. These authors also suggested that targeted therapies against CD9 and its downstream signals may be novel strategies for treating B-ALL. In addition, it has been revealed that CD9 is able to increase the ability of B-ALL cells to disseminate via RAC1 activation (18). In ALL, CD9 expression is correlated with the expression of the BCR-ABL fusion gene and indicates poor prognosis (19). Therefore, the present study investigated the effects of CD9 on the biological features of Ph^{+} ALL cells. In the present study, a loss-of-function approach was used to analyze the biological effect of CD9 in Ph^{+} ALL cells. A lentiviral shRNA expression vector targeting CD9 gene was constructed and used to transduce the Ph[+] ALL cell line SUP-B15. Silenced CD9 significantly inhibited SUP-B15 cell proliferation *in vitro*. From the flow cytometry analysis, it was demonstrated that the SUP-B15 apoptotic rate was significantly increased when the CD9 gene was knocked down. Cell cycle analysis demonstrated that CD9 knockdown caused G_2/M phase cell cycle to arrest in SUP-B15 cells. Taken together, these results from the *in vitro* experiments suggested

that the therapeutic suppression of CD9 expression may lead to inhibition of the progression of Ph⁺ ALL. However, in order to further evaluate the therapeutic effects of CD9 knockdown on Ph⁺ ALL *in vivo*, it is necessary to establish xenograft models of Ph⁺ ALL.

As a tumor suppressor protein, p53 has a key effect on balancing between cell proliferation and death by suppressing cell cycle progression via p21 upregulation and promoting apoptosis via caspase 3 activation (25,26). In the present study, it was identified that silenced CD9 upregulated protein expression levels of p53 and p21, which may result in the suppression of proliferation in SUP-B15 cells. In addition to attenuating proliferation, silenced CD9 also exhibited pro-apoptotic properties. However, the relatively high apoptosis in CD9-silenced SUP-B15 cells could be decreased by caspase 3 blocker (Z-DEVD-FMK). Thus, it was hypothesized that caspase 3, the executioner of cell death (27), may be involved in apoptosis induced by silenced CD9. Western blotting was used to analyze the expression of cleaved caspase 3, and the results demonstrated that the expression of cleaved caspase 3 was upregulated in the SUP-B15 cells transduced with CD9-shRNA.

Intensive multi-agent chemotherapy has produced a high complete remission rate in pediatric ALL (28). However, Ph⁺ ALL remains largely resistant to the currently available chemotherapy strategies (29). The CD9⁺ population of human precursor-B ALL cell lines has been identified to be relatively more chemotherapy-resistant than the CD9⁻ population (17). In the present study, it was found that silenced CD9 was able to increase VCR, DNR, CPM and DXM-induced cytotoxicity in SUP-B15 cells. These findings suggested that chemotherapy combined with knockdown of CD9 may be a novel potential approach for treating Ph⁺ ALL. It is possible that the combination of different anti-cancer strategies that disrupt different cell signaling pathways leads to enhanced destruction of cancer cells. The potential mechanisms of how CD9 knockdown may promote the efficacy of chemotherapeutic agents include, but are not limited to, the shared intracellular signaling pathways involved in cell cycle control, apoptosis or drug metabolism and efflux, which should be further investigated.

In patients with Ph⁺ ALL, the response to the selective BCR-ABL tyrosine kinase inhibitor imatinib is not as effective as in Ph⁺ CML (6), and the underlying biological mechanism remains largely unknown. The present study demonstrated that silenced CD9 promoted sensitivity to imatinib in SUP-B15 cells. These findings suggested that imatinib combined with knockdown of CD9 may be a promising strategy for treating Ph⁺ ALL.

Invasion and metastasis are key clinicopathological features of acute leukemia (23); therefore, identifying the mechanism involved in the dissemination of Ph⁺ ALL may lead to the development of novel and more effective treatment approaches. In the present study, silenced CD9 markedly suppressed cell adhesion, migration and invasion in SUP-B15 cells. These results suggested that CD9 may serve a key role involved in leukemic cell invasion and metastasis in Ph⁺ ALL. The present results are in line with other previous studies reporting that CD9 enhances metastatic medullary invasion of precursor-B leukemic cells *in vivo* (16,17), and that CD9

promotes the adhesion of leukemic B lymphocytes to fibronectin and the migration of these leukemic cells in response to C-X-C motif chemokine ligand 12 (18). These results suggested that therapeutic strategies involving CD9 gene silencing may inhibit the invasion and migration of Ph⁺ ALL cells, and lead to improved clinical outcome; however, further research is needed to determine the potential mechanisms of the CD9 molecule on cell motility in Ph⁺ ALL cells.

A limitation of the present study is that the experiments were only performed in the Ph⁺ ALL cell line SUP-B15. In contrast to cell lines, patient-derived primary leukemia cells reflect the heterogeneous nature of cancer biology, as they exist in patients. Thus, the potential anti-leukemia effect of gene silencing of CD9 using an shRNA expressing lentivirus vector should be further evaluated in primary Ph⁺ ALL cells. Moreover, despite high transduction efficiency in SUP-B15 cells obtained in the shRNA approach, only one of the three tested shRNA sequences significantly decreased the CD9 mRNA expression to ~26% compared with the shControl cells. RNA interference-mediated gene silencing technologies can suffer from pervasive off-target effects and non-specific toxicity (30-32). Therefore, further experiments using additional loss-of-function strategies with high on-target efficiencies and low off-target effects (such as CRISPR/Cas9-mediated gene knockout) will be required to elucidate the role of the CD9 gene in leukemogenesis in Ph⁺ ALL.

In conclusion, the present study demonstrated that the silencing of the CD9 gene induced apoptosis and G_2/M cell cycle arrest via a p53-dependent pathway in Ph⁺ ALL SUP-B15 cells. Additionally, the downregulation of CD9 expression inhibited the cell proliferation, adhesion, migration and invasion of SUP-B15 cells, and increased the efficacy of chemotherapeutic drugs and imatinib. Therefore, it was hypothesized that the genetic silencing of CD9 using an shRNA-expressing lentivirus vector may provide a promising treatment for Ph⁺ ALL.

Availability of data and materials

The datasets generated or analyzed during this study are not publicly available due to confidentiality of another study from our group but are available from the corresponding authors upon reasonable request.

Authors' contributions

JF and SG conceived of the project. CX, WX, YS, BZ, DW and BL conducted the experiments and collected the data. CX, WX, YS, YZ, SG and JF analyzed the data. CX, WX and

YS wrote the paper. All authors read and approved the final manuscript.

Ethics approval and consent to participate

Not applicable.

Patient consent for publication

Not applicable.

Competing interests

The authors declare that they have no competing interests.

References

1. Inaba H, Greaves M and Mullighan CG: Acute lymphoblastic leukaemia. Lancet 381: 1943-1955, 2013.
2. Bernt KM and Hunger SP: Current concepts in pediatric Philadelphia chromosome-positive acute lymphoblastic leukemia. Front Oncol 4: 54, 2014.
3. Fielding AK: How I treat Philadelphia chromosome-positive acute lymphoblastic leukemia. Blood 116: 3409-3417, 2010.
4. Pui CH, Sandlund JT, Pei D, Campana D, Rivera GK, Ribeiro RC, Rubnitz JE, Razzouk BI, Howard SC, Hudson MM, *et al*: Improved outcome for children with acute lymphoblastic leukemia: Results of total therapy study XIIIB at St Jude children's research hospital. Blood 104: 2690-2696, 2004.
5. Druker BJ, Guilhot F, O'Brien SG, Gathmann I, Kantarjian H, Gattermann N, Deininger MW, Silver RT, Goldman JM, Stone RM, *et al*: Five-year follow-up of patients receiving imatinib for chronic myeloid leukemia. N Engl J Med 355: 2408-2417, 2006.
6. Lee HJ, Thompson JE, Wang ES and Wetzler M: Philadelphia chromosome-positive acute lymphoblastic leukemia: Current treatment and future perspectives. Cancer 117: 1583-1594, 2011.
7. Maecker HT, Todd SC and Levy S: The tetraspanin superfamily: Molecular facilitators. FASEB J 11: 428-442, 1997.
8. Hemler ME: Tetraspanin functions and associated microdomains. Nat Rev Mol Cell Biol 6: 801-811, 2005.
9. Wang JC, Bégin LR, Bérubé NG, Chevalier S, Aprikian AG, Gourdeau H and Chevrette M: Down-regulation of CD9 expression during prostate carcinoma progression is associated with CD9 mRNA modifications. Clin Cancer Res 13: 2354-2361, 2007.
10. Zöller M: Tetraspanins: Push and pull in suppressing and promoting metastasis. Nat Rev Cancer 9: 40-55, 2009.
11. Peñas P, García-López M and del Río Barreiro O: Inhibition of the motility of melanoma cells using interference RNA against CD9. Actas Dermosifiliogr 96: 30-36, 2005 (In Spanish).
12. Herr MJ, Mabry SE, Jameson JF and Jennings LK: Pro-MMP-9 upregulation in HT1080 cells expressing CD9 is regulated by epidermal growth factor receptor. Biochem Biophys Res Commun 442: 99-104, 2013.
13. Wang GP and Han XF: CD9 modulates proliferation of human glioblastoma cells via epidermal growth factor receptor signaling. Mol Med Rep 12: 1381-1386, 2015.
14. Rappa G, Green TM, Karbanová J, Corbeil D and Lorico A: Tetraspanin CD9 determines invasiveness and tumorigenicity of human breast cancer cells. Oncotarget 6: 7970-7991, 2015.
15. Tang M, Yin G, Wang F, Liu H, Zhou S, Ni J, Chen C, Zhou Y and Zhao Y: Downregulation of CD9 promotes pancreatic cancer growth and metastasis through upregulation of epidermal growth factor on the cell surface. Oncol Rep 34: 350-358, 2015.
16. Nishida H, Yamazaki H, Yamada T, Iwata S, Dang NH, Inukai T, Sugita K, Ikeda Y and Morimoto C: CD9 correlates with cancer stem cell potentials in human B-acute lymphoblastic leukemia cells. Biochem Biophys Res Commun 382: 57-62, 2009.
17. Yamazaki H, Xu CW, Naito M, Nishida H, Okamoto T, Ghani FI, Iwata S, Inukai T, Sugita K and Morimoto C: Regulation of cancer stem cell properties by CD9 in human B-acute lymphoblastic leukemia. Biochem Biophys Res Commun 409: 14-21, 2011.
18. Arnaud MP, Vallée A, Robert G, Bonneau J, Leroy C, Varin-Blank N, Rio AG, Troadec MB, Galibert MD and Gandemer V: CD9, a key actor in the dissemination of lymphoblastic leukemia, modulating CXCR4-mediated migration via RAC1 signaling. Blood 126: 1802-1812, 2015.
19. Liang P, Miao M, Liu Z, Wang H, Jiang W, Ma S, Li C and Hu R: CD9 expression indicates a poor outcome in acute lymphoblastic leukemia. Cancer Biomark 21: 781-786, 2018.
20. Wu J, Liang B, Qian Y, Tang L, Xing C, Zhuang Q, Shen Z, Jiang S, Yu K and Feng J: Down-regulation of CD19 expression inhibits proliferation, adhesion, migration and invasion and promotes apoptosis and the efficacy of chemotherapeutic agents and imatinib in SUP-B15 cells. Cell Biol Int 42: 1228-1239, 2018.
21. Sanber KS, Knight SB, Stephen SL, Bailey R, Escors D, Minshull J, Santilli G, Thrasher AJ, Collins MK and Takeuchi Y: Construction of stable packaging cell lines for clinical lentiviral vector production. Sci Rep 5: 9021, 2015.
22. Livak KJ and Schmittgen TD: Analysis of relative gene expression data using real-time quantitative PCR and the 2(-Delta Delta C(T)) method. Methods 25: 402-408, 2001.
23. Klein G, Vellenga E, Fraaije MW, Kamps WA and de Bont ES: The possible role of matrix metalloproteinase (MMP)-2 and MMP-9 in cancer, eg acute leukemia. Crit Rev Oncol Hematol 50: 87-100, 2004.
24. Barrena S, Almeida J, Yunta M, López A, Fernández-Mosteirín N, Giralt M, Romero M, Perdiguer L, Delgado M, Orfao A and Lazo PA: Aberrant expression of tetraspanin molecules in B-cell chronic lymphoproliferative disorders and its correlation with normal B-cell maturation. Leukemia 19: 1376-1383, 2005.
25. Vogelstein B, Lane D and Levine AJ: Surfing the p53 network. Nature 408: 307-310, 2000.
26. Shen Y and White E: p53-dependent apoptosis pathways. Adv Cancer Res 82: 55-84, 2001.
27. Slee EA, Adrain C and Martin SJ: Serial killers: Ordering caspase activation events in apoptosis. Cell Death Differ 6: 1067-1074, 1999.
28. Kato M and Manabe A: Treatment and biology of pediatric acute lymphoblastic leukemia. Pediatr Int 60: 4-12, 2018.
29. Gleissner B, Gökbuget N, Bartram CR, Janssen B, Rieder H, Janssen JWG, Fonatsch C, Heyll A, Voliotis D, Beck J, *et al*: Leading prognostic relevance of the BCR-ABL translocation in adult acute B-lineage lymphoblastic leukemia: A prospective study of the german multicenter trial group and confirmed polymerase chain reaction analysis. Blood 99: 1536-1543, 2002.
30. Barrangou R, Birmingham A, Wiemann S, Beijersbergen RL, Hornung V and van Brabant Smith A: Advances in CRISPR-Cas9 genome engineering: Lessons learned from RNA interference. Nucleic Acids Res 43: 3407-3419, 2015.
31. Grimm D, Streetz KL, Jopling CL, Storm TA, Pandey K, Davis CR, Marion P, Salazar F and Kay MA: Fatality in mice due to oversaturation of cellular microRNA/short hairpin RNA pathways. Nature 441: 537-541, 2006.
32. Kaelin WG Jr: Use and abuse of RNAi to study mammalian gene function. Science 337: 421-422, 2012.